

Detection of Gaseous and Particulate Fluorides by Laser-Induced Breakdown Spectroscopy

MICHAEL TRAN, BENJAMIN W. SMITH, DAVID W. HAHN, and
JAMES D. WINEFORDNER*

Departments of Chemistry and Mechanical Engineering, University of Florida, Gainesville, Florida 32611-7200

Laser-induced breakdown spectroscopy (LIBS) was evaluated for the detection of gaseous and particulate fluorides in air and other gas mixtures. Analytical figures of merit were compared in pure air, pure He, air-He mixtures, and air with a He sheath flow. Particulate samples were also collected on filters and subsequently detected. It was demonstrated that SF₆ is a suitable surrogate for calibration and optimization for the detection of HF in air. For gaseous F in air, limits of detection obtained were 40 mg/m³ for the direct measurement in air and 5 mg/m³ when the air sample was sheathed in He. For particulate F in air, limits of detection were 9 mg/m³ for direct measurement in air and 0.5 mg/m³ using He sheath flow. When the particulates were pre-concentrated by collection on a filter and subsequently analyzed, the limit of detection for F was improved to 5 µg/m³ for a 10-min sampling time at 10 L/min flow rate using subsequent LIBS measurements in pure He.

Index Headings: Laser-induced breakdown spectroscopy; LIBS; Fluoride; Aerosols.

INTRODUCTION

Fluoride emissions are an important concern in the aluminum processing industry for both environmental and economic reasons. Depending on concentration, both gaseous and particulate fluorides can be toxic to plants and animals and are subject to regulatory controls by both federal and state agencies. Particulate emissions result primarily from pot tending practices, whereby fine particulates, mostly in the form of sodium aluminum fluoride, are released into the ventilation hood system during surface crust breaking activities.

Real-time monitoring of both gaseous and particulate fluoride emissions can lead to improved smelting practice and thus to reduced total fluoride emissions and more economical aluminum production. Because of such benefits, the U.S. Environmental Protection Agency (EPA) continues to encourage facilities to evaluate the use of real-time emissions monitoring technologies. A reduction in fluoride emissions and improvements in the efficiency of the aluminum production process have been identified as important national goals in a recent Department of Energy (DOE) report.¹ While several techniques (e.g., FT-IR and diode laser absorption) exist for the real-time measurement of gaseous fluoride, primarily as HF, there are no practical methods available for real-time monitoring of fluoride emission in the form of particulates. The method commonly employed is to collect the sample with a filter followed by digestion and dissolution. The resulting liquid sample is then analyzed by conventional techniques such as mass spectrometry, chromatography,

or fluoride-selective electrode. These methods are rather tedious, time consuming, and prone to error due to the many steps in sample handling. More significantly, such off-line methods do not lend themselves to process optimization and real-time feedback. Laser-induced breakdown spectroscopy (LIBS), on the other hand, is rapid, *in situ*, and requires little or no sample preparation. In addition, samples can be solids, liquids, or gases, with small amounts (micrograms) required for the analysis.

BACKGROUND

Laser-induced breakdown spectroscopy has been of interest ever since the invention of the pulsed ruby laser in 1961. Any pulsed laser of more than a few mJ pulse energy, when focused to produce an irradiance of greater than about 10 MW cm⁻², will produce a breakdown and form an energetic plasma in most solids, liquids, and gases. The process is exceedingly complex and dependent upon the local environment, the nature of the laser-material interaction, and the laser pulse energy, duration, temporal and spatial character, and wavelength. The plasma emission spectrum is characteristic of the vaporized, atomized, and excited elemental species present in the vicinity of the breakdown event and can be used for both qualitative and quantitative analysis. Although LIBS has many inherent advantages as an analytical method, many problems remain with regard to accuracy, precision, and detection power. Recent technological developments, mainly the availability of fast, sensitive, gated multichannel detectors (e.g., charge-coupled devices), echelle spectrometers, and reliable, compact pulsed laser sources (especially compact Nd:YAG lasers), have made the technique increasingly practical. During the last 15 years or so, a wide variety of applications have appeared ranging from industrial process monitoring and quality control to the detection of heavy metals in soils, paints, and solid organic and environmental samples. LIBS has been applied for the analysis of gases, fluids, and aerosols, molten metals, polymeric material, and many types of solids.²⁻⁷

For aerosol analysis, the laser-induced microplasma is both the sample volume and the excitation source for LIBS-based analysis. All molecules and fine particulates (roughly 10 µm and smaller) are atomized and excited efficiently within the highly energetic microplasma. The resulting plasma emission can be resolved both spectrally and temporally to yield atomic emission spectral lines corresponding to the atoms present in the plasma volume. The LIBS technique has been used for the analysis of a wide range of particulate species and compounds, including metal hydrides, coal particles, and the elements alu-

Received 6 February 2001; accepted 4 July 2001.

* Author to whom correspondence should be sent.

minum, arsenic, beryllium, cadmium, chromium, calcium, fluorine, iron, lead, magnesium, manganese, mercury, nickel, and others in a variety of samples.

Hahn et al. have demonstrated that LIBS can be used to monitor real-time particulate emissions in several processes. Field demonstrations include real-time measurements of sodium and calcium in the exhaust duct of a 200 ton/day glass furnace, as well as measurements of particulate metals in the effluent streams of hazardous waste incinerators and military ordnance destruction facilities.^{8,9} Their recent research has successfully extended the LIBS technique for quantitative analysis of individual particles.¹⁰

Neuhauser et al. have recently developed a mobile system, consisting of a 19 in. rack with a laser and spectrometer/detector module connected to a miniaturized sensor head through fiber optics, for direct analysis of automatically acquired aerosols on a sample filter.¹¹ Similarly, Zhang et al. have developed and tested a mobile LIBS system as a multimetal continuous emission monitor during a joint U.S. DOE-EPA test, which measured concentrations of Cr, Pb, Cd, and Be in near real time.¹²

The detection of gaseous halogen compounds has been demonstrated by several investigators. In 1983, Cremers and Radziemski reported the detection of Cl and F in air using LIBS with limits of detection of 8 and 38 ppm (w/w), respectively.¹³ Two different groups, Williams et al.¹⁴ and Lancaster et al.,¹⁵ used a Nd:YAG LIBS system to detect halogenated fire suppressants such as C₃F₇H and CF₄. Typical limits of detection were several hundred ppm by weight. More recently, Haich et al. reported on the detection of chlorine containing gases with limits of detection in the low ppm range.¹⁶

EXPERIMENTAL

Instrumental Setup. The experimental setup for LIBS has been described,¹⁷ so only a brief description will be given. It consisted of a laser, a motorized x, y, z translational stage carrying the sample, a spectrometer, an intensified charged-coupled device (ICCD) detector (Princeton Instruments, USA, 384 × 576 pixels), detector gating and control electronics, and a computer for control and data acquisition. A Nd:YAG laser (Quantel Brilliant, France) with a 100 mJ laser pulse energy at the fundamental wavelength of 1064 nm, a 5 ns pulse duration, and 1 Hz repetition frequency was used in this study. A 1200 groove/mm grating, with a blaze wavelength of 750 nm, was installed to obtain a larger spectral window (17 nm) and accessibility to the near IR region. The best spectral resolution obtained was 0.05 nm.

For gas or aerosol detection, a sample chamber was designed as shown in Fig. 1. A 1064 nm bestform lens, with a focal length of 2 cm and a diameter of 1.3 cm, was mounted on the side of the chamber with the higher convex surface facing the laser beam. A 0.5 cm diameter collection lens was mounted on the top of the chamber to direct the LIBS emission to the spectrometer via a fiber optic bundle. An outlet at the side of the chamber, not shown in Fig. 1, was connected to a ventilation system. A two-layer inlet tube designed to produce sheath or laminar flow was mounted at the bottom. The inner and outer tube sizes (i.d.) were 2.5 mm and 5 mm, respectively.

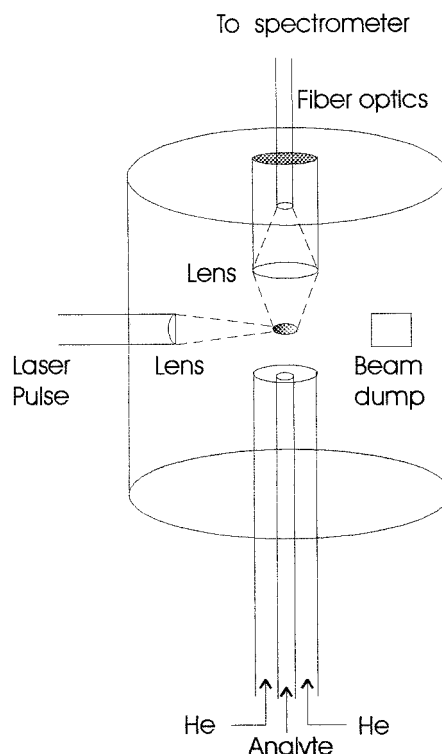


FIG. 1. Schematic of the sample chamber.

For solids detection, a simple plastic box (3 × 3 × 1 in.) containing no F compounds was designed for quick and easy sample access and handling. It included a quartz window mounted on the top of the box facing the laser beam to allow laser ablation and detection of emission, an inlet on one side of the box, which was connected to the He gas source, and two separate outlets on the other side. Before each measurement, He gas was flushed through the chamber at a rate of 10 L/min to purge most of the air, whereas during each measurement, the flow rate of He was reduced to 3 L/min to maintain a stable plasma. Test results indicated that there was no detectable air present in the chamber during the LIB measurement. This method was very quick and efficient compared to the use of a vacuum.

For measurements of particulates on the filter membrane, the target was moved horizontally between shots so that each laser sampling was on a fresh location to improve the reproducibility of mass ablation. An optimized measurement gate delay time of 0.6 μs and an integration time of 10 μs were used for all analyses. Each sample measurement consisted of 3 or 4 replicates with an accumulation of 20 laser shots per replicate. The net analyte signal intensity was calculated by subtracting the average background signal intensity from the average signal obtained for the total laser shots. The background signal intensity was the average intensity taken on the two sides of the analyte peak.

Samples and Sample Preparation. In this study, SF₆ (Specialty Chemical Products, Inc.) was used as a substitute for HF since SF₆ is relatively inexpensive and non-toxic. We will demonstrate that SF₆ is a suitable surrogate for optimization and calibration for the detection of HF by LIBS. To produce a calibration curve, 0.1% (v/v) cer-

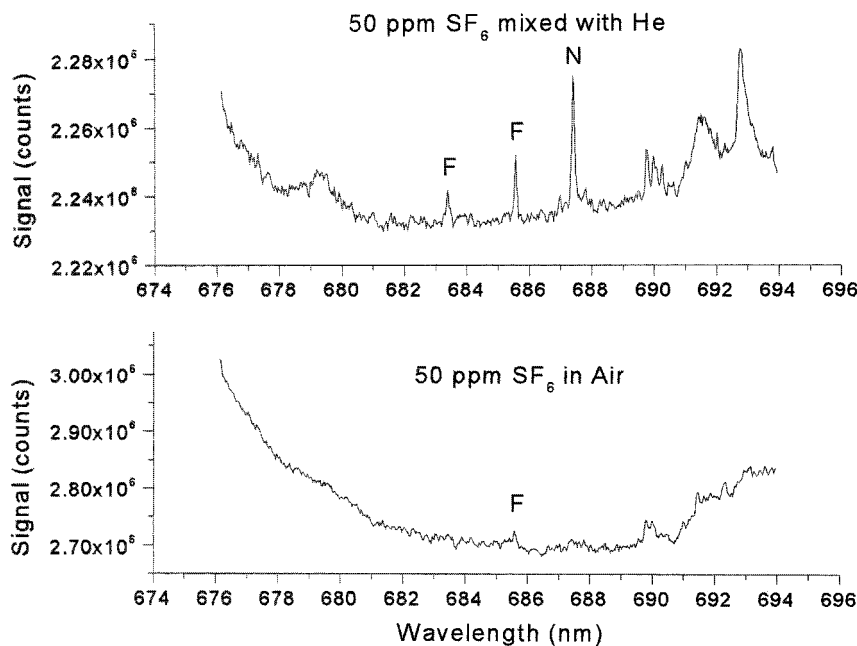


FIG. 2. Spectra of 50 ppm SF₆ in air and He atmosphere at delay and gate times of 0.6 μs and 10 μs, respectively. Each spectrum is the accumulation of 100 laser pulses.

tified SF₆ was diluted with air in different ratios. To ensure the accuracy of the dilution, a digital flowmeter (Optiflow 650, Humonics Inc.) with a precision of better than 2% was used.

Sodium fluoride aerosol was generated using an ultrasonic nebulizer (U-6000AT+, CETAC Technologies). Standard NaF solutions, prepared by diluting NaF (Alfa Aesar, 99%) with deionized water, were pumped into the nebulizer using a peristaltic pump.

Another indirect sampling technique involved collection of F particulate on a filter. An aqueous 10 000 ppm F solution, prepared from NaF powder, was nebulized in air using a pneumatic nebulizer at a rate of 0.1 mL/min. The F aerosol mass concentration was calculated to be 21 μg/L in the gaseous flow stream. The aerosols were then collected on ultra-thin, high performance membrane filters (0.02 μm pore size, 2 cm diameter, Alltech) for 5, 10, and 15 min using a vacuum pump, which produced an air flow rate of 10 L/min through the filter, as sampled from the 21 μg/L aerosol flow stream. The size of the particulate F particles was on the order of 100 nm, based on TEM analysis of a number of other particle types similarly produced.

RESULTS AND DISCUSSION

Buffer Gas. The surrounding atmosphere has a great influence on the emission characteristics of a laser-induced plasma. Plasma emission in air has the drawbacks of intense background continuum and self-absorbed, broadened spectral lines. Noble gas environments have been used in several LIBS applications and studies. Argon gas at atmospheric pressure was used in our lab as a buffer in the determination of C:H:O:N ratios of solid organic compounds.¹⁸ Singh et al. have shown an improvement of 2.5 times in the limit of detection (LOD) of Sn by using He buffer gas.¹⁹ Iida has studied the effect of argon at reduced atmosphere and found the signal in-

tensity increased 20 times compared to air.²⁰ However, this increase in signal intensity was accompanied by an increase in the background intensity. Aguilera et al.²¹ have found that temperatures and electron densities were higher in Ar and lower in He compared with air. The use of a buffer gas has only been applied to solid analysis. One drawback of using a buffer gas for gas or aerosol analysis is that the analyte will be diluted.

In this study, two approaches to the use of a buffer gas were examined. The first approach was to mix the analyte flow stream with a buffer gas prior to introducing it into the sample chamber. The second was to use a concentric sampling tube, which produced a flow of analyte concentrated in the center and surrounded by a sheath buffer gas. Figure 2 clearly shows a significant enhancement in S/N ratio of the F emission line at 685.6 nm by mixing the 50 ppm SF₆ (in air) with He, even though the analyte was greatly diluted by He. The spectral background is lower for measurements in He (2.23 E6 counts) than in air (2.70 E6 counts). This results because helium has a higher thermal conductivity than air and therefore suppresses the background continuum from the plasma. The spectrum of 50 ppm SF₆ (in air) mixed with He (Fig. 2) also shows an emission line at 687.4 nm, which is hardly seen in the spectrum in air. We suspect that it came from nitrogen since it appears only when a small amount of nitrogen or air is mixed with He gas. Since it was not the focus of this study, we did not investigate this matter further. We also made a similar study using Ar gas as a buffer, but there was no significant improvement in the S/N ratio.

Delay Time. Figure 3 shows the emission spectra of SF₆ at different delay times at a fixed gate width of 0.1 μs. At very early times in the formation of the plasma in air, the signal is mostly dominated by the continuum background and background noise, as illustrated by the top spectrum in Fig. 3. The continuum gradually dimin-

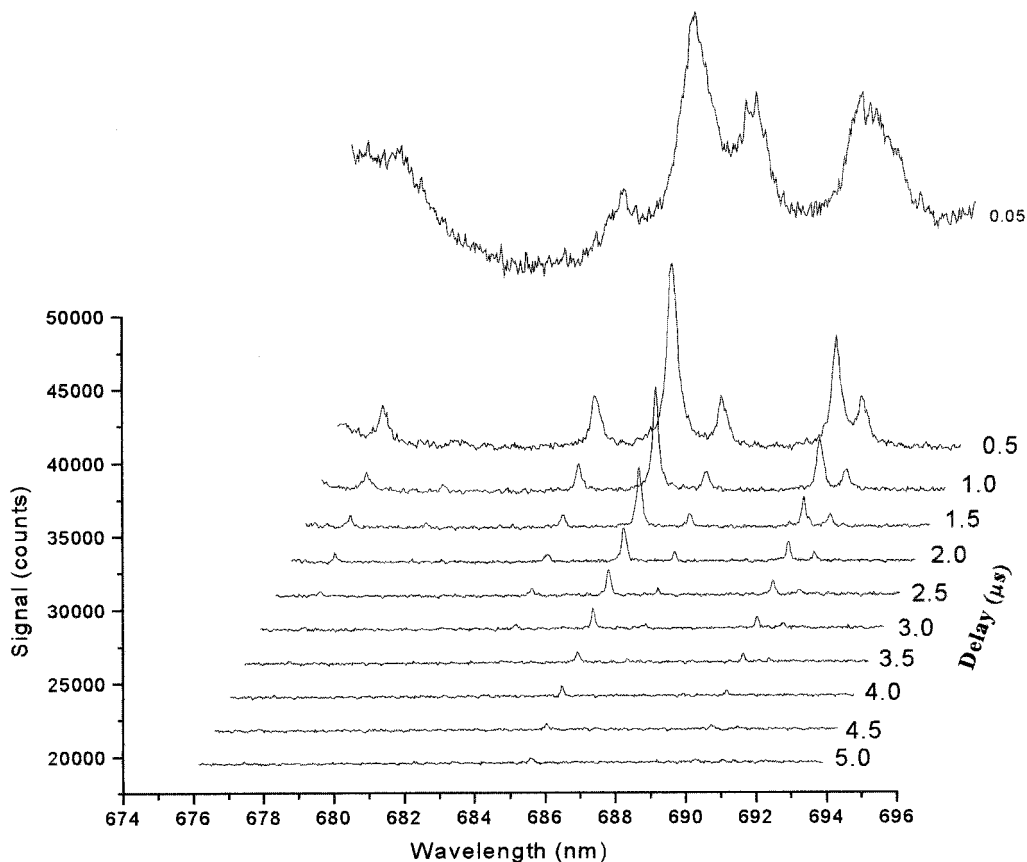


Fig. 3. Single shot spectra of SF₆ in air at different delay times. The gate time was kept constant at 0.1 μs.

ishes as the emission line evolves. To obtain the best result, the delay time, which is the time between the beginning of a laser pulse and data acquisition, must be optimized. Figure 4 shows a plot of the F signal against the gate delay time in different atmospheres. SF₆ was premixed with air, oxygen, and nitrogen at a fixed ratio of 6:100, whereas it was premixed with helium at a ratio of 1:100, before being introduced into the chamber. One hundred successive shots were programmed by the pulse generator during which the gate delay was varied from 0.05 to 5.05 μs with a fixed gate width of 0.1 μs. The emission profile of fluorine in N₂ is similar to that in air, as expected. The F emission profiles in N₂ and O₂ are similar in that they exhibit a maximum at a delay time of 0.6 μs. However, F emission intensity in O₂ is higher than in N₂ or air, suggesting that the excitation process in O₂ is more efficient than in N₂.

The emission behavior of F in He is different than in N₂ and O₂ in terms of both intensity and time. As shown in Fig. 4, the F emission in He forms at a very early time and drops approximately exponentially during the first few μs and then almost linearly. After 5 μs, while the F signal in air is greatly diminished, the F signal in He still remains high and in fact persists beyond 10 μs. The high intensity and longevity of the F emission intensity in He is most likely a result of the inertness of the He medium, as it minimizes combination of F with other atoms to form molecular species. Other characteristics of the F spectrum in He include low background continuum and narrow emission linewidth, which are related to the high thermal conductivity of He, as it cools down the plasma

quicker than air or Ar. One potential application of the low continuum background of the He plasma is that the gated ICCD detector could be replaced by a simple CCD, and therefore the LIBS system could be less expensive and more compact.

Detection of Gaseous Fluoride. Choice of Standard.

Gaseous HF is one of the main fluoride emissions from aluminum processing. However, since it is highly irritating, corrosive, and poisonous, SF₆ gas was substituted in our study. SF₆ is inert, non-toxic, and relatively inexpensive. To check the assumption that SF₆ is a suitable surrogate for HF, the LIBS fluorine signal for a 600 ppm (v/v) HF was measured and compared with the signal given by 100 ppm (v/v) of SF₆. These would provide equivalent concentrations of F in the laser probe volume. They produced nearly identical LIBS signals for fluorine, as shown in Fig. 5. This finding is consistent with previously reported work that demonstrates the nominal independence of elemental emission on the molecular source.²²

Helium Flow Optimization. As mentioned earlier, the F signal to noise ratio (SNR) increases significantly in the presence of He. The spectrum noise is taken as the standard deviation of a portion of the background next to the signal. A typical LOD for fluorine reported in the literature was in the range of 40 ppm (w/w), or 60 ppm (v/v).^{13,15,23,24} From now on, we will refer to ppm always as part per million by volume for all gaseous fluorides. In this study, we tried to lower the LOD by two approaches. In the first approach, the SF₆ standard was mixed directly with He before introduction into the cham-

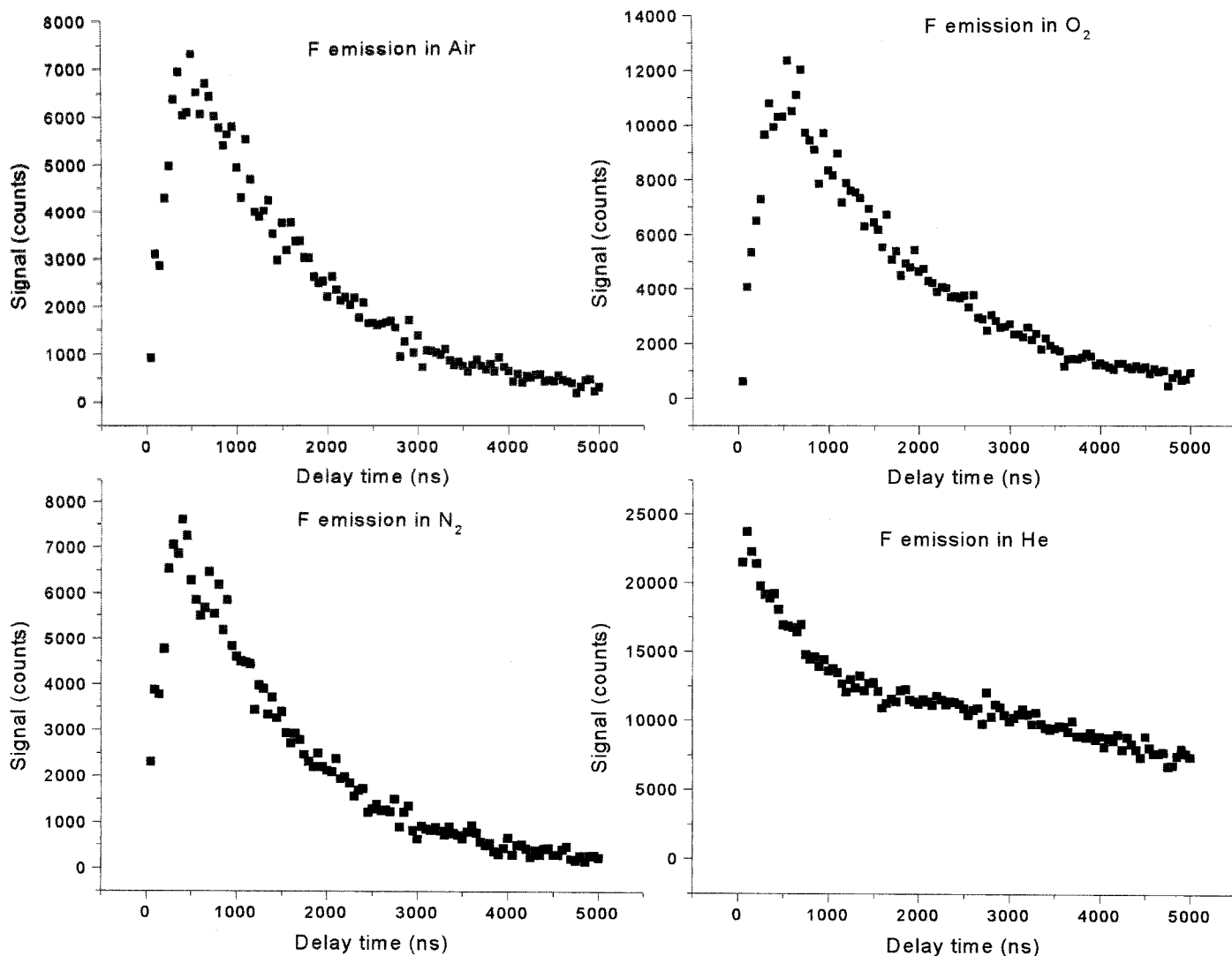


FIG. 4. Emission profiles of F in different atmospheres. The gate time was kept constant at 0.1 μ s.

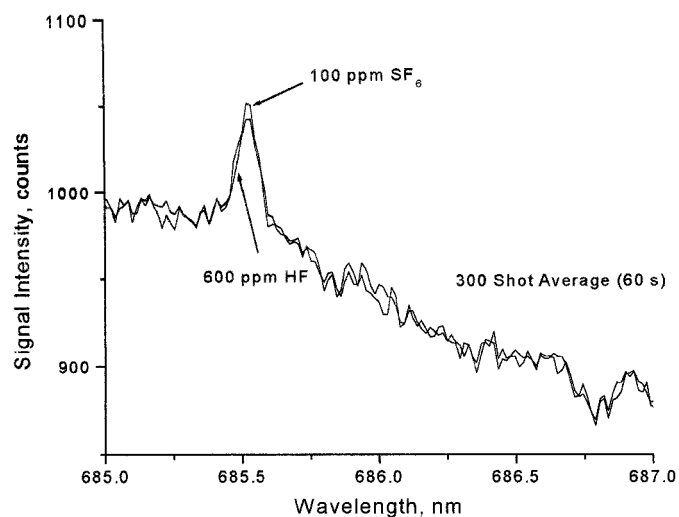


FIG. 5. Comparison of the F emission spectra of equivalent [F] due to SF₆ and HF.

ber. Figure 6 shows a plot of fluorine emission SNR as a function of He flow rate. This was done by keeping the air-diluted SF₆ standard flow constant at 1 L/min while varying the flow rate of He. The optimum SNR was obtained at a He flow rate of about 5 L/min. Even though the SF₆ sample was diluted by six times, a 4-fold enhancement in SNR was observed.

In the second approach, a concentric tube was designed to produce a laminar flow sheath around the sample stream as described in the experimental section. The SF₆/air sample was contained within the He sheath gas stream. Figure 7 shows a plot of fluorine emission SNR as a function of He flow rate. Interestingly, there were two maxima at flow rates of 5 L/min and 13 L/min, while the sample flow rate was kept constant at 1 L/min. We suspect that at low flow rates, the sample and He mixed together, resulting in a 4-fold improvement at 5 L/min flow rate similar to the sample and helium premixing shown in Fig. 6. At higher flow rates, a sheath flow formed, where He still mixed with the sample flow but prevented dilution of the sample flow by the surroundings. An 8-fold enhancement was obtained at a He flow rate of 13 L/min.

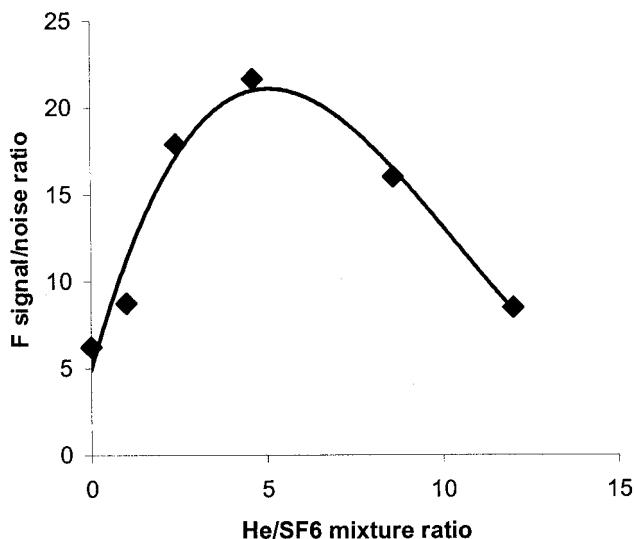


FIG. 6. Optimization of the He to sample ratio.

Detection of Particulate Fluoride. Particulate Generation. Particulate fluoride was generated by an ultrasonic nebulizer, which produced sub-micrometer particles from standard NaF solutions. The concentration of F aerosol was calculated by:

$$C_{\text{aerosol}} = \epsilon \frac{C_{\text{solution}} \times F_{\text{solution}}}{F_{\text{gas}}} \quad (1)$$

where C_{aerosol} is the concentration of F in the aerosol (mg/L), ϵ is the nebulizer efficiency, C_{solution} is the F solution concentration (mg/mL), F_{solution} is the sample uptake (mL/min), and F_{gas} is the gas flow rate (L/min). The nebulizer efficiency ϵ (the fraction of NaF aerosol entering the sample chamber, accounting for losses in transport) was calibrated by bubbling aerosol into a flask containing deionized water and calculated as:

$$\epsilon = \frac{C_{\text{in}}}{C_{\text{out}}} \quad (2)$$

where C_{in} is the concentration of NaF solution after the aerosol was bubbled into the flask, and C_{out} is the concentration of the standard NaF solution, which was nebulized for a period of time so that the volume withdrawn is the same as that of the deionized water in the flask. The NaF concentration, C_{in} was then determined by monitoring the Na emission line at 589 nm and double-checked by conductance measurements. To examine the concentration dependency of the nebulizer, five different NaF concentrations were studied. No significant variation in the nebulizer efficiency was observed. The average nebulizer efficiency was 4%.

Limits of Detection. The limits of detection of gaseous and particulate fluorides for different conditions and setups are given in Table I. The lowest LOD was obtained in pure He, more than two orders of magnitude better than that in air. However, this figure of merit is for reference only since it has no real practical application for direct gaseous or particulate detection since air cannot be totally eliminated from the sample. The LOD for gaseous fluorine in air, which is 40 mg/m³ (48 ppm w/w), is comparable to values reported in literature.^{13,15,23,24} By mixing

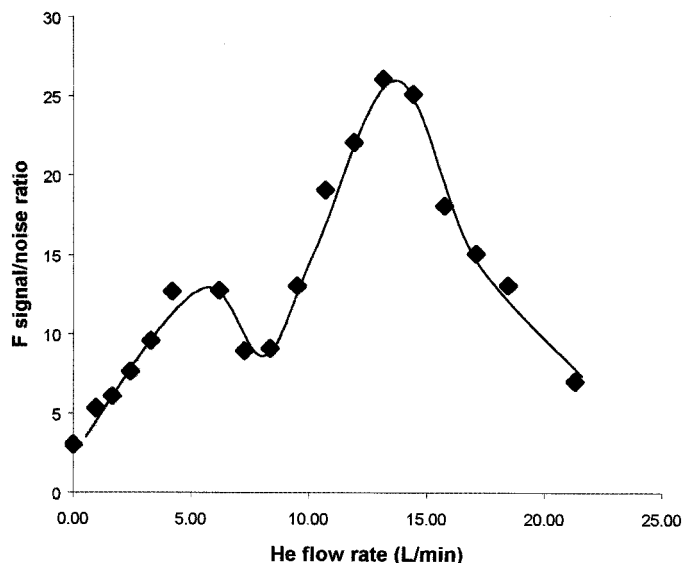


FIG. 7. Optimization of the He flow rate in a sheath flow tube.

with He or using the sheath flow tube, we demonstrated that F can be detected in the low ppm range. Limits of detection for the aerosol are significantly lower than for the gaseous fluoride. This is understandable since the electron number density for plasma-containing aerosols, especially with the presence of an easily ionized element, such as Na, is typically higher than that for pure gasses.²⁵ In light of this, the introduction of any aerosol into a sample gas should improve the detection limit for gaseous samples.

Detection of Particulate Fluorides on a Filter. Since the LODs of gaseous F are different from those of particulate F , and currently the LIBS technique cannot distinguish whether the signal comes from the gas or particulates, it is difficult to quantify a sample without prior knowledge of its constituents. One approach to quantifying gaseous and particulate fluorides separately is to collect the aerosol onto a filter, which is a common means for aerosol sampling. The gaseous fluoride passing through the filter could then be subjected to direct LIBS analysis. After a desired period of time, the aerosol on the filter could be analyzed on-site or off-site by LIBS.

To construct the calibration curve, aerosols generated by a pneumatic nebulizer were collected on a filter for different periods of time, as described in the Experimental section. Because of the efficiency of the filter, we assume that all particles are captured. The fluorine density in terms of $\mu\text{g}/\text{cm}^2$ of F on the filter was calculated as:

TABLE I. Limits of detection (mg/m³) of gaseous and particulate fluorides analyzed in different atmospheres. The delay and gate times are 0.6 μs and 10 μs , respectively.

	Air	Mix with He ^a	He sheath flow ^b	Pure He ^c
Gaseous	40	10	5	0.3
Particulate	9	1	0.5	0.1

^a LODs were calculated based on concentration of F in air before mixing. The actual concentration after mixing with He was 5–10 times lower.

^b Sample and He co-flow in a concentric tube.

^c No air in sample.

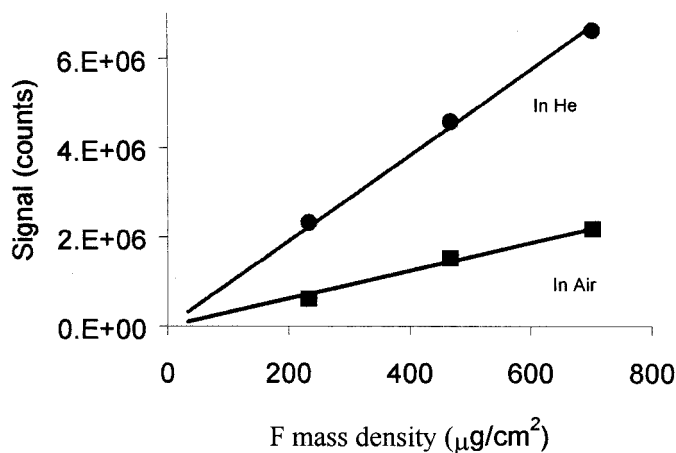


FIG. 8. Calibration curves of F aerosol collected on a filter with the collection times of 5, 10, and 15 min and analyzed in air and He atmospheres.

$$D_f = \frac{C_{\text{aerosol}} \times F \times t_c}{A_f} \quad (3)$$

where C_{aerosol} is the F concentration in the aerosol in $\mu\text{g/L}$, F is the flow rate of air passed through the filter in L/min , t_c is the collection time in minutes, and A_f is the area of the filter in cm^2 .

Figure 8 shows the calibration curves of fluoride particulate on filters in air and He at atmospheric pressure. Both curves are linear and pass through the origin, indicating that no interference or self-absorption occurred. Each data point is the accumulated signal of 20 laser shots on the filter. As expected, the F spectrum in He resulted in much higher signals and lower background noise. Therefore, the LOD of fluorine is lower in He than in air by a factor of 15, as shown in Table II. The LOD in terms of $\mu\text{g/m}^3$ was calculated based on an average 10 min collection time and a gas sampling flow rate of 10 L/min . Increasing the collection time or flow rate will decrease the LOD proportionally. Compared with direct aerosol analysis, this technique improved the LOD by more than 50 times. The LOD for F in particulates was $5 \mu\text{g/m}^3$ or 4 ppb (w/w) in He. In addition to the 10 min collection time, the analysis turn-around time is less than 15 min, which is near real time, as compared with conventional techniques, which might take hours, if not days.

CONCLUSION

We have demonstrated that LIBS is a promising technique in the detection and monitoring of gaseous and particulate fluorides in air. The advantages of this technique include little or no sample preparation, speed, low cost, and suitability for on-line or near real-time monitoring in industrial and environmental applications. In this study, helium proved to be the best plasma medium for fluorine detection. The LODs are improved by 4 and 8 times, respectively, by either mixing or sheath co-flowing of He with gaseous or particulate samples. Detection of aerosol using filters followed by LIBS analysis is still

TABLE II. Limits of detection of particulate fluorides collected on a filter and analyzed in air and He atmospheres. The delay and gate times are $0.6 \mu\text{s}$ and $10 \mu\text{s}$, respectively.

LIPS gas	$\mu\text{g/cm}^2$	pg/shot	$\mu\text{g/m}^3$ ^a
Air	2.4	230	75
He	0.16	16	5.0

^a Based on a sampling volume of 0.1 m^3 and a loaded filter area of 3.1 cm^2 .

very desirable, especially for applications requiring low limits of detection.

ACKNOWLEDGMENTS

Financial support by the National Science Foundation Engineering Research Center (NSF-ERC) for Particle Science and Technology at the University of Florida and the Industrial Partners of the ERC is gratefully acknowledged. This work was also supported by the University of Florida Opportunity Fund and a grant from Alcoa. The authors would like to thank Dr. Neal Dando and Dr. Igor B. Gornushkin for helpful discussions and Mr. Luis Espinoza-Nava for the HF sample set up.

- Aluminum Industry Technology Roadmap, U.S. DOE, May, 1997.
- I. B. Gornushkin, J. E. Kim, B. W. Smith, S. A. Baker, and J. D. Winefordner, *Appl. Spectrosc.* **51**, 1055 (1997).
- B. J. Marquardt, S. R. Goode, and S. M. Angel, *Anal. Chem.* **68**, 977 (1996).
- D. A. Rusak, B. C. Castle, B. W. Smith, and J. D. Winefordner, *Crit. Rev. Anal. Chem.* **27**, 257 (1997).
- M. Tran, Q. Sun, B. W. Smith, and J. D. Winefordner, *Anal. Chim. Acta* **419**, 153 (2000).
- R. Wisbrun, I. Schechter, R. Niessner, H. Schroder, and K. L. Kompa, *Anal. Chem.* **66**, 2964 (1994).
- A. Ciucci, V. Palleschi, S. Rastelli, R. Barbini, F. Colao, R. Fantoni, A. Palucci, S. Ribezzo, and H. J. L. van der Steen, *Appl. Phys. B* **63**, 185 (1996).
- D. W. Hahn, *Appl. Phys. Lett.* **72**, 2960 (1998).
- S. G. Buckley, H. A. Hohnsen, K. R. Hencken, and D. W. Hahn, *Waste Management* **20**, 455 (2000).
- D. W. Hahn and M. M. Lunden, *Aerosol Sci. and Technol.* **33**, 30 (2000).
- R. E. Neuhauser, U. Panne, and R. Niessner, *Anal. Chim. Acta* **392**, 47 (1999).
- H. Zhang, F.-Y. Yueh, and J. P. Singh, *Appl. Opt.* **38**, 1459 (1999).
- D. A. Cremers and L. J. Radziemski, *Anal. Chem.* **55**, 1252 (1983).
- E. D. Lancaster, K. L. McNesby, R. G. Deniel, and A. W. Miziolek, *Appl. Opt.* **38**, 1476 (1999).
- C. K. Williamson, R. G. Deniel, K. L. McNesby, and A. W. Miziolek, *Anal. Chem.* **70**, 1186 (1998).
- C. Haich, R. Niessner, O. I. Matveev, U. Panne, and N. Omenetto, *Fresenius' J. Anal. Chem.* **356**, 21 (1996).
- Q. Sun, M. Tran, B. W. Smith, and J. D. Winefordner, *Anal. Chim. Acta* **143**, 187 (2000).
- M. Tran, Q. Sun, B. W. Smith, and J. D. Winefordner, *J. Anal. At. Spectrom.*, paper submitted.
- J. P. Singh, H. Zhang, F.-Y. Yueh, and K. P. Carney, *Appl. Spectrosc.* **50**, 764 (1996).
- Yasuo Iida, *Appl. Spectrosc.* **43**, 229 (1989).
- J. A. Aguilera and C. Aragon, *Appl. Phys. A* **69**, (Suppl.) S475 (1999).
- M. Essien, L. J. Radziemski, and J. Sneddon, *J. Anal. At. Spectrom.* **3**, 985 (1988).
- T. R. Loree, L. J. Radziemski, and D. A. Cremers, *Electro-optical System Design*, Oct 1982, 35–41.
- L. Dudragne, Ph. Adam, and J. Amouroux, *Appl. Spectrosc.* **52**, 1321 (1998).
- J. D. Ingle and S. R. Crouch, *Spectrochemical Analysis* (Prentice Hall, Englewood Cliffs, 1988), p. 201.